MECHANIKA TEORETYCZNA
I STOSOWANA
Journal of Theoretical
and Applied Mechanics
4, 31, 1993

THE STOCHASTIC SIMULATION OF A VISCOUS FLOW PAST AN AIRFOIL – PART II, NUMERICAL CALCULATIONS

JANUSZ BŁAŻEWICZ

ANDRZEJ STYCZEK

Institute Of Aeronautics and Applied Mechanics
Warsaw University of Technology

The present contribution consists in a detailed description of the algorithm emerging from the principles given in our previous paper (Blażewicz and Styczek, 1993). Methods of determination of the decomposed velocity field components, together with the methods of the blobs position fixing have been presented. One can find in the paper also some methods of the computer visualization.

1. Introduction

The scheme of stochastic simulation of a fluid flow algorithm supplied with the theoretical basis was presented in the previous part of this paper. In the present part we will turn to the details concerning particular problems appearing in the algorithm realization process, i.e. geometrical description of the motion being under consideration (airfoil, flow area), evaluation of coefficients and right-hand sides of the equations describing the new blobs circulations, determination of both the total flow velocity and blobs motion in accordance with the Ito equations. The crucial point for the present algorithm realization was application of the computer of a relatively small power to numerical calculations (i.e. IBM PC/AT microcomputer supplied with the Definicon accelerator card), which forced us to introduce unusual numerical techniques at certain stages of the process, e.g. spreading a network over a flow area and interpolating some velocity components within it, as well as employing the so-called substitute blobs. Both the aforementioned methods tended to reduce a number of operations performed at one time step.

Another troublesome question, not so directly connected with the computer efficiency, was the problem of increasing number of blobs with the simulation time passing by due to the way of the blobs creation on an airfoil contour at the inverse

mechanism (disintegration of blobs) being written off the algorithm. It is obvious that there exist the natural limit for the simulation time – up till the moment at which the number of blobs increases to the value disallowing further calculations for either the long time or the computer power required. It turned out, that due to the algorithm being employed the simulation time required for the correct calculations would be rather relatively long one.

We have assumed that the simulation process starts with the flow in which the vorticity appears only within the areas close to the airfoil contour i.e. at the initial moment only the first generation of blobs exists. It has been also assumed that the simulation is realized over the period of time needed for the blobs to flow down a distance of a several chords from the airfoil, what needs a lot of time steps to be realized. At each step the number of blobs remaining in the flow increases with the network (employed to the approximation of the boundary vorticity distribution) spread over an airfoil density gettinghigher. At a high number of blobs remaining on the boundary – hundreds of them – the total number of them appearing during the simulation could reach a few or several thousand, which obviously would exceed the computer capacity. It was necessary then to introduce – despite of the process of blobs creation on the airfoil boundary – the mechanism of the total number of blobs existing in a flow reduction, which was achieved due to the operation of the blobs summing up.

Let us assume that due to stochastic components of the process, centers of different blobs are located close enough. The vorticity within the areas created by circles bounding the blobs is a single-valued function having a form of sum of the component vorticities. Shapes of these areas are determined by the radii and distances between the overlapping blobs, respectively. Induction in the far exterior of the system created in such a way will not change significantly when the lumped vortex of the global circulation will substitute for it. A small-range interaction appears as a result of the superposition described above and can be determined with acceptable approximation in terms of a small-range induction of a substitute blob having the largest radius and exhibiting a circulation being a sum of the component circulations.

The aforementioned operation, performed at different "intensity levels" – higher far from an airfoil and minimal in the airfoil vicinity – enables one to control the total number of blobs and keep it at the level adequate to the computer power.

The process of summing up blobs despite of its main role i.e. reduction of a blobs number within the flow, has also been applied to creation of the aforementioned substitute blobs systems. These are auxiliary systems (of less components) formed for the successive stages of calculations, in which the summation of the intensity distributed over the motion area has been performed in a way ensuring the calculation time reduction without any influence on the calculations quality.

It is obvious that the aforementioned operations aiming at the calculations

flowchart optimization escape from the analysis of their influence on the simulation results quality. It was assumed, however, that they were necessary and both the realization and the parameter choice were based on the results observation.

2. Geometrical relations

Let us name a plane of an airfoil the flow plane z.

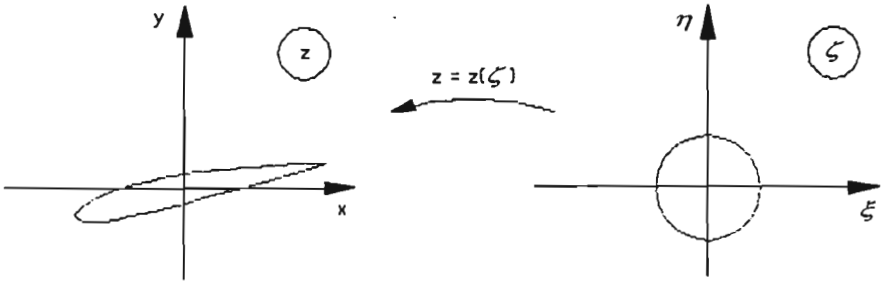

Fig. 1.

The contour of the airfoil under consideration appears as a result of the unit circle transformation, center of which is located at the point (0,0) lying on the ζ plane, performed in terms of the following function having a form of series

$$z = z(\zeta) = \zeta + c_0 + \sum_{k=1}^{K} \frac{c_k}{\zeta^k} \tag{2.1}$$

where the coefficients $c_0, c_1, ..., c_K$ are known.

Let us divide the circle into N parts, each one of which has to be divided next into L segments. The point defining this division have the following arguments

$$\begin{aligned} &\theta_0^j = j\Delta\theta_N && j = 0, 1, ..., N \\ &\theta_k^j = j\Delta\theta_N + k\Delta\theta && j = 0, 1, ..., N-1 \qquad k = 0, 1, ..., L \end{aligned} \tag{2.2}$$

where

$$\Delta\theta_N = \frac{2\pi}{N} \qquad \Delta\theta = \frac{\Delta\theta_N}{L}$$

It is obvious that

$$\theta_0^N = \theta_0^0 + 2\pi$$

and

$$\theta_L^j = \theta_0^{j+1} \qquad \text{for} \quad j = 0, 1, ..., N-1$$

It would be convenient to employ a common index for the points enumeration

$$l = jL + k$$

for $j = 0, 1, ..., N-1$, $k = 0, 1, ..., L-1$ and for $j = N$, $k = 0$.

One can write then

$$\theta_l = l\Delta\theta \qquad l = 0, 1, ..., NL \tag{2.3}$$

in particular it is $\theta_0 = \theta_{NL} - 2\pi$.

The following proper airfoil contour division can be then defined by means of the transformation (2.1)

$$P_k^j = z\left(e^{i\theta_k^j}\right) \qquad \text{or} \qquad P_l = z\left(e^{i\theta_l}\right)$$

The points P_0^j, $j = 0, 1, ..., N$ represent the ends of N segments, over which new blobs will appear. We assume that the center B_k ($k = 1, 2, ..., N$) of each segment has to be located over the center of $P_0^{k-1}P_0^k$ segment at a distance of half its length

$$B_k = \frac{1}{2}\left(P_0^{k-1} + P_0^k\right) + \frac{1}{2}\left(P_0^k - P_0^{k-1}\right)e^{-i\frac{\pi}{2}}$$

The bounding circle of the blob has a radius σ_k chosen in a way ensuring intersection of an airfoil at points P_0^{k-1}, P_0^k, respectively

$$\sigma_k = \frac{1}{\sqrt{2}}\left|P_0^k - P_0^{k-1}\right|$$

The airfoil arc s measured from the trailing point is a function of the θ angle defined on the circle in an usual way.

It can be written

$$\frac{dz}{d\theta} = \frac{dz}{d\zeta}\Big|_{\zeta \subset K} \frac{d}{d\theta}\left(e^{i\theta}\right) = ie^{i\theta}\frac{dz}{d\zeta}\Big|_{\zeta \subset K} \tag{2.4}$$

Let β denote the angle between the $0X$ axis and the unit vector tangent to an airfoil t. We can write

$$\frac{dz}{d\theta} = \frac{ds}{d\theta}e^{i\beta} \tag{2.5}$$

One can achieve then

$$\frac{ds}{d\theta} = \left|\frac{dz}{d\theta}\right| = \left|\frac{dz}{d\zeta}\right|_{\zeta \subset K} \tag{2.6}$$

After integrating Eq (2.6), under the additional condition $s(0) = 0$, one can determine the function $s(\theta)$. The right-hand side of Eq (2.6) is calculated at the

points $\zeta = \exp(i\theta_l)$, $l = 0, 1, ..., NL$, directly from the formula for transformation derivative

$$\frac{dz}{d\zeta} = 1 - \frac{1}{\zeta}\sum_{k=1}^{K}\frac{kc_k}{\zeta^k} \tag{2.7}$$

Applying the trapezoidal rule to integration we arrive at

$$\begin{aligned} s_0 &= 0 \\ s_l &= s_{l-1} + \frac{1}{2}\Delta\theta\Big[\frac{ds}{d\theta}(\theta_{l-1}) + \frac{ds}{d\theta}(\theta_l)\Big] \qquad l = 1, 2, ..., NL \end{aligned} \tag{2.8}$$

Eqs (2.4) and (2.5) will be also applied to determination of the unit vector t tangent to the airfoil points. The following formula holds

$$t = e^{i\beta} = \frac{\frac{dz}{d\theta}}{\frac{ds}{d\theta}} = \frac{ie^{i\theta}\frac{dz}{d\zeta}\Big|_{\zeta\subset K}}{\Big|\frac{dz}{d\zeta}\Big|_{\zeta\subset K}}$$

One can calculate then

$$t_l = t(\theta_l) \qquad l = 0, 1, ..., NL \tag{2.9}$$

The tangent unit vectors $t = e^{i\beta}$ can be employed in determination of tangent and normal velocity components, respectively. One can write

$$v^t - iv^n = (u - iv)e^{i\beta} = (u - iv)t \tag{2.10}$$

or

$$v^t + iv^n = (u + iv)e^{-i\beta} = (u + iv)\frac{1}{t}$$

For purposes of the blobs displacement control we define a network spread over the airfoil exterior. Components of the velocity fields, including the component induced by the blobs, will be calculated at the network nodes. Interpolating the total velocity calculated at these points we will arrive velocity components at the blob center. Calculating the blob center velocity in the aforementioned, indirect way, we can reduce significantly the calculation time, especially if the number of network nodes is considerably lower than the number of blobs.

The second important role, which the network plays, is enabling the plain verification whether the blob has already crossed the area boundary (the airfoil contour or hypothetical outer boundary) or not.

The last, but not least, role of the network is giving the possibility of quick "picking up" the neighboring groups of blobs from the variety of blobs existing within the flow (by means of controling the correlation between the current blob number and the closest network nodes numbers).

The advantages of the network application are obvious, having in mind the aforementioned functions of it:

- relatively small number of nodes,
- high concentration of nodes in the vicinity of an airfoil.

Such a network appears as a result of the conformal transformation (2.1) applied to the proper network spread over the unit circle outwards. The points, at which half-lines emanating from the coordinate system origin at ϑ_j angles relative the 0ξ axis intersect the circles of radius r_i concentric with the unit circle, create the auxiliary network.

Denoting this network nodes by $\zeta_{i,j}$ we write

$$\zeta_{i,j} = r_i e^{i\vartheta_j} \tag{2.11}$$

From the assumption of the uniform circuit division into $N_S - 1$ segments it follows

$$\begin{aligned} &\vartheta_1 = 0 \\ &\vartheta_j = \vartheta_{j-1} + \Delta\vartheta \qquad\qquad j = 2, 3, ..., N_S \end{aligned}$$

where $\Delta\vartheta = 2\pi/(N_S - 1)$.

It is worth noting that $\vartheta_{N_S} = \vartheta_1 + 2\pi$.

The formulae for r_i radii read

$$\begin{aligned} &r_1 = 1 \\ &r_i = r_{i-1}(1 + W_i) \qquad\qquad i = 2, 3, ..., N_W \end{aligned}$$

For $W_i = 1$ the distance between the successive points of the $i-1$ layer, measured along the arc, represents the distance between the layers i and $i-1$, respectively. Through the proper choice of the W_i value, compression or decompression of a grid, respectively, in the radial direction can be obtained.

It is convenient to evaluate W_i using the formula

$$W_i = A(i-1) + B$$

For the proper concentration of nodes to be obtained near the airfoil the following two ranges of layers are introduced:

- the near one, containing N_{WB} layers,
- the distant range with all the remaining layers.

In each of these ranges different pairs of parameters A and B are determined.

The transformation (2.1) of the auxiliary plane enables us to represent the network spread over the airfoil exterior nodes $z_{i,j}$ by the points $\zeta_{i,j}$. Nodes of the first layer $(z_{1,j})$ are located on the airfoil contour and the both the ends of each layer overlap i.e. $z_{i,1} = z_{i,N_S}$.

The coordinates of the network nodes can be calculated from the following formula (in accordance with Eq (2.1))

$$z_{i,j} = r_i e^{i\vartheta_j} + c_0 + \sum_{k=1}^{K} \frac{c_k}{r_i^k e^{ik\vartheta_j}} \qquad \begin{matrix} i = 1, 2, ..., N_W \\ j = 1, 2, ..., N_S \end{matrix}$$

We calculate also at each node the transforming function derivative (which may be employed e.g. to the $\vec{V}_p$ velocity determination)

$$\frac{dz}{d\zeta}(z_{i,j}) = 1 - \frac{1}{r_i e^{i\vartheta_j}} \sum_{k=1}^{K} \frac{kc_k}{r_i^k e^{ik\vartheta_j}}$$

The scheme of the network spread over the airfoil is give in Fig.2

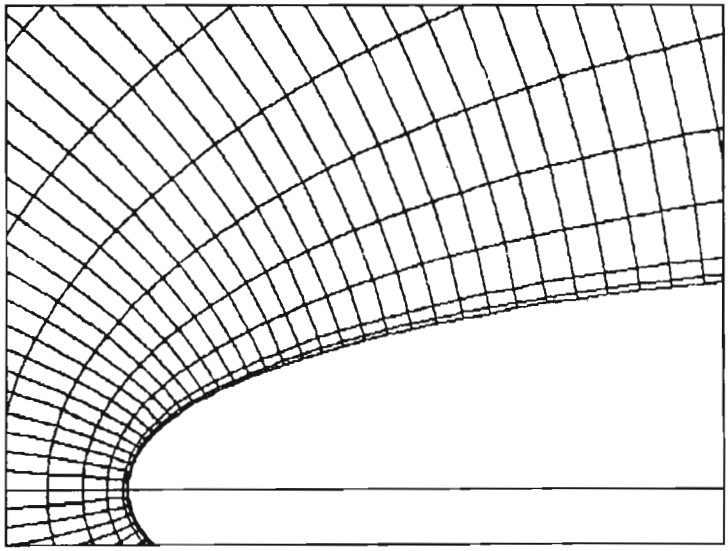

Fig. 2.

The scheme of the network spread over the airfoil, with the location of just appearing blobs being marked is given in Fig.3.

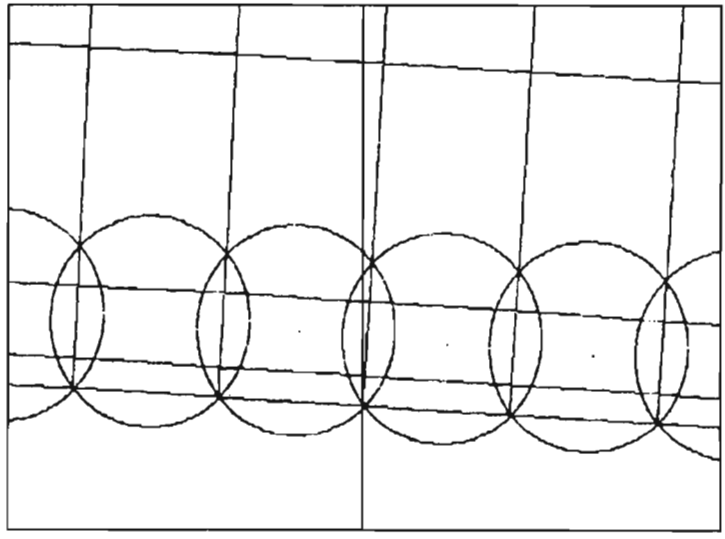

Fig. 3.

3. Velocity fields $\vec{V}_p$, $\vec{V}_\Gamma$

$\vec{V}_p$ represents the velocity of an inviscid fluid flow past the airfoil under consideration. Let us employ the well-known conformal transformation (cf e.g. Prosnak, 1970).

Let the velocity at infinity be $V_\infty = U_\infty e^{i\alpha}$ while the circle radius $a = 1$. The following complex potential represents a solution to the aforementioned problem

$$W(\zeta) = V_{z\infty}\zeta + \frac{\Gamma}{2\pi i}\ln\zeta + V_\infty\frac{1}{\zeta}$$

where

$$V_{z\infty} = U_\infty e^{-i\alpha}$$

The circulation Γ should be chosen in a way ensuring that one of the two impact points appearing on a circle is located at the point (1,0) representing the inverse image of the airfoil cusp.

To this end let us write the formula for a complex velocity

$$V_{zp} = \frac{dW}{d\zeta} = V_{z\infty} + \frac{\Gamma}{2\pi i\zeta} - V_\infty\frac{1}{\zeta^2} \tag{3.1}$$

under condition that it vanishes at the point $\zeta = (1,0)$. Thus we obtain (Fig.4)

$$V_{zp}(\zeta) = U_\infty\left(1 - \frac{1}{\zeta}\right)\left(e^{-i\alpha} + \frac{e^{i\alpha}}{\zeta}\right) \tag{3.2}$$

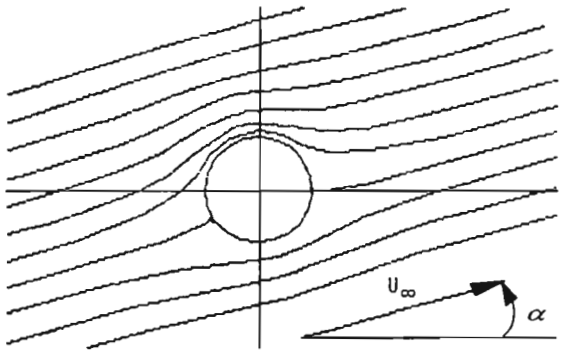

Fig. 4.

The formula for the corresponding complex velocity in the flow plane z can be written as

$$V_{zp}(z) = V_{zp}(\zeta)\Big(\frac{dz}{d\zeta}\Big)^{-1} \tag{3.3}$$

while the sought-for velocity $\vec{V}_p$, being a conjugate reads

$$V_p(z) = \mathrm{conjg} V_{zp}(z) \tag{3.4}$$

Having in mind Eq (2.10) we calculate the tangent component V_p^t of the velocity $\vec{V}_p$ on an airfoil

$$V_p^t(z)\Big|_{\text{airfoil}} = V_p^t(s) = \mathrm{re}\Big[V_{zp}(z)t\Big] = \mathrm{re}\Big[\mathrm{i}e^{\mathrm{i}\theta}V_{zp}(\zeta)\Big(\frac{ds}{d\theta}\Big)^{-1}\Big] \tag{3.5}$$

The velocity $V_\Gamma(z)$, in turn, corresponds (in terms of the transformation $z = z(\zeta)$) with the velocity field of the potential vortex with circulation Γ and located at the circle center lying in the auxiliary plane.

The complex velocity induced by the aforementioned vortex can be written

$$V_{z\Gamma}(\zeta) = \frac{dW_\Gamma}{d\zeta} = \frac{\Gamma}{2\pi\mathrm{i}\zeta}$$

Thus in the flow plane we have

$$V_{z\Gamma}(z) = V_{z\Gamma}(\zeta)\Big(\frac{dz}{d\zeta}\Big)^{-1} \tag{3.6}$$

while as in the previous case

$$V_\Gamma(z) = \mathrm{conjg} V_{z\Gamma}(z)$$

Let us calculate the tangent and normal components of $\vec{V}_\Gamma$ on an airfoil. Applying the relation

$$V_r - \mathrm{i}V_\theta = V_z(\zeta)\mathrm{e}^{\mathrm{i}\theta}$$

for $\zeta = \mathrm{e}^{\mathrm{i}\theta}$ we can write

$$V_{r\Gamma} - \mathrm{i}V_{\theta\Gamma} = V_{z\Gamma}\left(\zeta = \mathrm{e}^{\mathrm{i}\theta}\right)\mathrm{e}^{\mathrm{i}\theta} = -\frac{\Gamma\mathrm{i}}{2\pi}$$

i.e.

$$V_{r\Gamma} = 0 \qquad V_{\theta\Gamma} = \frac{\Gamma}{2\pi} \tag{3.7}$$

which, having in mind the well-known relation (cf Błażewicz and Styczek, 1993) enables us to determine

$$V_\Gamma^n = 0 \qquad V_\Gamma^t = \frac{\Gamma}{2\pi}\left(\frac{ds}{d\theta}\right)^{-1} \tag{3.8}$$

4. Calculations of the blobs circulation

Solution to the equation set given in the previous part (cf Błażewicz and Styczek, 1993 – Eqs (3.32) and (3.33)) determines the circulation of still appearing blobs, while the matrix $\mathbf{R}$ entries read

$$R_{jk} = \int_{s_0^{j-1}}^{s_0^j} \mathcal{L}N(s,k)ds - \int_{s_0^{j-1}}^{s_0^j} T(s,k)ds + \int_{s_0^{j-1}}^{s_0^j} V_l^t(s)ds = r_{jk}^1 + r_{jk}^2 + r_{jk}^3 \tag{4.1}$$

$$j,k = 1,2,...,N$$

The components r_{jk}^1, r_{jk}^2, r_{jk}^3 have to be calculated.

Functions $N(s,k)$ and $T(s,k)$ represent the normal and tangent components, respectively, of the velocity induced on the airfoil (at the point $P(s)$) by the blob of unit circulation, center of which is located at the point B_k (over the $P_0^{k-1}P_0^k$ segment). Substituting for $\Gamma = 1$ and defining the points B_k and $P(s_l) = P_l$ coordinates, respectively, we can rewrite the induction formula (cf Błażewicz and Styczek, 1993 – Eq (3.28)) as follows

$$u(s_l,k) + \mathrm{i}v(s_l,k) = \begin{cases} \dfrac{\mathrm{i}}{2\pi}\dfrac{P_l - B_k}{\sigma_k^2} & \text{for } |P_l - B_k| \le \sigma_k \\ \dfrac{\mathrm{i}}{2\pi}\dfrac{P_l - B_k}{|P_l - B_k|^2} & \text{for } |P_l - B_k| \ge \sigma_k \end{cases} \tag{4.2}$$

Applying Eq (2.10) one obtains

$$T(s_l,k)+\mathrm{i}N(s_l,k)=[u(s_l,k)+\mathrm{i}v(s_l,k)]\frac{1}{t_l} \tag{4.3}$$

at each point s_l of the airfoil, $l=0,1,...,NL$.

According to the formulae given in the Part I (Błażewicz and Styczek, 1993 – Eqs (3.43) and (3.44)) the first component appearing in Eq (4.1) reads

$$r^1_{jk}=-\frac{1}{\pi}\int_0^{\text{periphery}} N(s,k)\ln\left|\frac{\sin\frac{\theta(s_0^j)-\varphi(s)}{2}}{\sin\frac{\theta(s_0^{j-1})-\varphi(s)}{2}}\right|ds$$

or after evaluating the radial velocity on a circle lying in the auxiliary plane $H(\theta,k)$, corresponding to $N(s,k)$ (see Błażewicz and Styczek, 1993 – Eq (3.41)) we arrive at

$$\begin{aligned} H(\theta,k)&=-N(s,k)\frac{ds}{d\theta}\\ r^1_{jk}&=\frac{1}{\pi}\int_0^{2\pi} H(\varphi,k)\ln\left|\frac{\sin\frac{\theta(s_0^j)-\varphi}{2}}{\sin\frac{\theta(s_0^{j-1})-\varphi}{2}}\right|d\varphi \end{aligned} \tag{4.4}$$

The integrand appearing in Eq (4.4) is a discontinous function at

a) $\varphi=\theta_0^{j-1}$ $\varphi=\theta_0^j$

and for

b) $\varphi=0$ for $j=N$ $(\theta_0^N=2\pi)$

c) $\varphi=2\pi$ for $j=1$ $(\theta_0^{j-1}=\theta_0^0=0)$

The cases b) and c) are in fact particular situations of a) and therefore all of them can be considered together.

Let us see how to calculate the integral appearing in Eq (4.4) for $j\neq 1$ and $j\neq N$. For the sake of simplicity let us introduce the following notation

$$R(\varphi,j)\overset{\text{def}}{=}\ln\left|\frac{\sin\frac{\theta(s_0^j)-\varphi}{2}}{\sin\frac{\theta(s_0^{j-1})-\varphi}{2}}\right|$$

After a proper division of the integration range, having the points $\varphi=\theta_0^{j-1}$, $\varphi=\theta_0^j$ together with their close neighborhood drawn out, one can write

$$r_{jk}^1 = \frac{1}{\pi}\int_0^{\theta_0^{j-1}-\Delta\theta} H(\varphi,k)R(\varphi,j)d\varphi + \frac{1}{\pi}\int_{\theta_0^{j-1}-\Delta\theta}^{\theta_0^{j-1}+\Delta\theta} H(\varphi,k)R(\varphi,j)d\varphi +$$
$$+ \frac{1}{\pi}\int_{\theta_0^{j-1}+\Delta\theta}^{\theta_0^{j}-\Delta\theta} H(\varphi,k)R(\varphi,j)d\varphi + \frac{1}{\pi}\int_{\theta_0^{j}-\Delta\theta}^{\theta_0^{j}+\Delta\theta} H(\varphi,k)R(\varphi,j)d\varphi +$$
$$+ \frac{1}{\pi}\int_{\theta_0^{j}+\Delta\theta}^{2\pi} H(\varphi,k)R(\varphi,j)d\varphi$$

where $\Delta\theta = 2\pi/(NL)$, according to the division (2.2).

Let us denote the components of the sum given above as I_1, I_2, I_3, I_4, I_5, respectively.

The integrals I_1, I_3, I_5 are to be calculated numerically by means of the trapezoidal rule, e.g.

$$I_1 = \frac{\Delta\theta}{\pi}\Big[\sum_{p=0}^{j-2}\sum_{q=0}^{L-1} H(\varphi_q^p,k)R(\varphi_q^p,j) -$$
$$- \frac{1}{2}H(\varphi_0^0,k)R(\varphi_0^0,j) - \frac{1}{2}H(\varphi_{L-1}^{j-2},k)R(\varphi_{L-1}^{j-2},j)\Big]$$

The integrals I_2, I_4 are calculated approximately and having in mind that intervals of integration of the length $2\Delta\theta$ may be considered as the short ones and the function $H(\varphi,k)$ is continuous some values may be obtained in an analytical way.

For the values applied to calculations $N \sim 100$, $L \sim 4$ it can be written

$$\Delta\theta \sim \frac{2\pi}{400} \qquad \Delta\theta_L = L\Delta\theta \sim \frac{2\pi}{100}$$

So the integral I_4 can be rewritten in the form of sum

$$I_4 = I_{41} + I_{42} = \frac{1}{\pi}\int_{\theta_0^{j}-\Delta\theta}^{\theta_0^{j}+\Delta\theta} H(\varphi,k)\ln\Big|\sin\frac{\theta_0^j-\varphi}{2}\Big|d\varphi -$$
$$- \frac{1}{\pi}\int_{\theta_0^{j}-\Delta\theta}^{\theta_0^{j}+\Delta\theta} H(\varphi,k)\ln\Big|\sin\frac{\theta_0^{j-1}-\varphi}{2}\Big|d\varphi$$

The integral I_{41} is a singular one due to vanishing of the logarithm base at $\varphi = \theta_0^j$. Under the assumptions given above we can write

$$I_{41} \cong \frac{1}{\pi} H(\theta_0^j, k) \int_{\theta_0^j - \Delta\theta}^{\theta_0^j + \Delta\theta} \ln \left| \sin \frac{\theta_0^j - \varphi}{2} \right| d\varphi$$

and substituting for $\varphi - \theta_0^j = 2\alpha$ we arrive at

$$\begin{aligned} I_{41} &\cong \frac{2}{\pi} H(\theta_0^j, k) \int_{-\frac{\Delta\theta}{2}}^{\frac{\Delta\theta}{2}} \ln |\sin \alpha| d\alpha \cong \frac{2}{\pi} H(\theta_0^j, k) \int_{-\frac{\Delta\theta}{2}}^{\frac{\Delta\theta}{2}} \ln |\alpha| d\alpha = \\ &= \frac{4}{\pi} H(\theta_0^j, k) \int_0^{\frac{\Delta\theta}{2}} \ln \alpha d\alpha = \frac{4}{\pi} H(\theta_0^j, k) \Big[\frac{\Delta\theta}{2} \Big(\ln \frac{\Delta\theta}{2} - 1 \Big) - \\ &- \lim_{\varepsilon \to 0} \varepsilon (\ln \varepsilon - 1) \Big] = \frac{2}{\pi} H(\theta_0^j, k) \Delta\theta \Big(\ln \frac{\Delta\theta}{2} - 1 \Big) \end{aligned}$$

The integral I_{42} is calculated by means of the trapezoidal rule at the points $\varphi_1 = \theta_0^j - \Delta\theta$, $\varphi_2 = \theta_0^j$, $\varphi_3 = \theta_0^j + \Delta\theta$

$$\begin{aligned} I_{42} &\cong -\frac{1}{\pi} H(\theta_0^j, k) \Delta\theta \Big[\ln \Big| \sin \frac{\theta_0^{j-1} - \theta_0^j + \Delta\theta}{2} \Big| + \\ &+ \ln \Big| \sin \frac{\theta_0^{j-1} - \theta_0^j}{2} \Big| + \frac{1}{2} \ln \Big| \sin \frac{\theta_0^{j-1} - \theta_0^j - \Delta\theta}{2} \Big| \Big] \cong \\ &\cong -\frac{1}{\pi} H(\theta_0^j, k) \Delta\theta \Big[\ln \frac{(L-1)\Delta\theta}{2} + \ln \frac{L\Delta\theta}{2} + \frac{1}{2} \ln \frac{(L+1)\Delta\theta}{2} \Big] \end{aligned}$$

Assuming $\sqrt{L^2 - 1} \cong L$ one obtains

$$I_{42} \cong -\frac{2}{\pi} H(\theta_0^j, k) \Delta\theta \ln \frac{L\Delta\theta}{2}$$

and

$$\begin{aligned} I_4 &\cong -\frac{2}{\pi} H(\theta_0^j, k) \Delta\theta \Big(-\ln \frac{\Delta\theta}{2} + 1 + \ln \frac{L\Delta\theta}{2} \Big) = \\ &= -\frac{2}{\pi} H(\theta_0^j, k) \Delta\theta (\ln L + 1) = -4 H(\theta_0^j, k) \frac{1}{NL} (\ln L + 1) \end{aligned}$$

The integral I_2 is calculated in a similar way.

Calculations of r_{jk}^1 at $j = 1$ or $j = N$ are made in the same way.

The current element r^2_{jk} after evaluation of $T(s_l,k)$ at the airfoil points can be calculated directly applying the trapezoidal rule

$$\begin{aligned} r^2_{jk} &= -\int_{s_0^{j-1}}^{s_0^j} T(s,k)ds \cong -\frac{1}{2}\sum_{p=1}^{L}\Big[T(s_p^{j-1},k)+T(s_{p-1}^{j-1},k)\Big]\Big(s_p^{j-1}-s_{p-1}^{j-1}\Big) = \\ &= -\Big[\frac{1}{2}T(s_0^{j-1},k)\Big(s_1^{j-1}-s_0^{j-1}\Big)+\frac{1}{2}T(s_L^{j-1},k)\Big(s_L^{j-1}-s_{L-1}^{j-1}\Big)+ \\ &+ \sum_{q=1}^{L-1} T(s_q^{j-1},k)\Big(s_{q+1}^{j-1}-s_{q-1}^{j-1}\Big)\Big] \end{aligned} \tag{4.5}$$

It should be noticed that the tangent component V_1^t of velocity induced on an airfoil by the connected unit vortex appears in the formula for r^3_{jk}. In accordance with Eq (3.8) we can write

$$V_1^t(s) = \frac{1}{2\pi}\Big(\frac{ds}{d\theta}\Big)^{-1}$$

Then it is obvious that

$$\begin{aligned} r^3_{jk} &= \int_{s_0^{j-1}}^{s_0^j} V_1^t(s)ds = \frac{1}{2\pi}\int_{s_0^{j-1}}^{s_0^j}\Big(\frac{ds}{d\theta}\Big)^{-1}ds = \frac{1}{2\pi}\int_{\theta_0^{j-1}}^{\theta_0^j} d\theta = \\ &= \frac{1}{2\pi}\Big(\theta_0^j-\theta_0^{j-1}\Big) = \frac{L\Delta\theta}{2\pi} \end{aligned} \tag{4.6}$$

Since the matrix $\mathbf{R}$ remains unchanged it can be calculated once and transposed outside the main calculations course.

Entries of the right-hand side vector $\mathbf{B}$ given in the Part I (cf Błażewicz and Styczek, 1993 – Eq(3.32)) are defined by the following formulae

$$\begin{aligned} B_j &= \int_{s_0^{j-1}}^{s_0^j}\Big(V_p^t(s)+V_0^t(s)\Big)ds - \int_{s_0^{j-1}}^{s_0^j}\mathcal{L}V_0^n(s)ds - \Gamma_0\int_{s_0^{j-1}}^{s_0^j} V_1^t(s)ds = \\ &= b_j^1+b_j^2+b_j^3 \qquad\qquad j=1,2,...,N \end{aligned} \tag{4.7}$$

The component V_p^t of the potential velocity appearing in the formulae given above can be calculated applying Eq (3.5).

The velocity $\vec{V}_0$ can be represented at the points P_l of an airfoil by the sum of velocities induced at these points by the blobs both already existing and still

arriving in the flow. If we enumerate these blobs with the aid of integers $1,...,M$, denoting the centers by B_m, the following formula holds

$$\vec{V}_0(P_l) = \sum_{m=1}^{M} \Big[u(s_l,m) + \mathrm{i}v(s_l,m)\Big] \tag{4.8}$$

where the components $u(s_l,m), v(s_l,m)$ appear according to the induction formula (cf Blażewicz and Styczek, 1993 – Eq (3.28)), which now takes the following form

$$u(s_l,m) + \mathrm{i}v(s_l,m) = \begin{cases} \dfrac{\mathrm{i}\Gamma_m}{2\pi}\dfrac{P_l - B_m}{\sigma_m^2} & \text{for } |P_l - B_m| \le \sigma_k \\ \dfrac{\mathrm{i}\Gamma_m}{2\pi}\dfrac{P_l - B_m}{|P_l - B_m|^2} & \text{for } |P_l - B_m| \ge \sigma_m \end{cases} \tag{4.9}$$

Having the components $V_p^t(s)$, $V_0^t(s)$ already calculated at the point s_l of the airfoil, we can calculate the first term of Eq (4.7) applying the same procedure as to r_{jk}^2 calculation

$$\begin{aligned} b_j^1 \;\cong\; & \frac{1}{2}\Big[V_p^t(s_0^{j-1}) + V_0^t(s_0^{j-1})\Big]\Big(s_1^{j-1} - s_0^{j-1}\Big) + \\ + \; & \frac{1}{2}\Big[V_p^t(s_p^{j-1}) + V_0^t(s_L^{j-1})\Big]\Big(s_L^{j-1} - s_{L-1}^{j-1}\Big) + \\ + \; & \sum_{q=1}^{L-1}\Big[V_p^t(s_q^{j-1}) + V_0^t(s_q^{j-1})\Big]\Big(s_{q+1}^{j-1} - s_{q-1}^{j-1}\Big) \end{aligned}$$

In the same way, having the component $V_0^n(s_l)$ known, we can calculate the term b_j^2.

The last component b_j^3, according to Eq (4.6) reads

$$b_j^3 = -\Gamma_0 \frac{L\Delta\theta}{2\pi}$$

where Γ_0 represents the sum of circulations of all the previous generations of blobs.

To calculate circulations of the new generation blobs the procedure given below should be followed:

- initial (only once) calculations of the $\mathbf{R}^{-1}$ matrix together with the tangential component V_p^t at the airfoil points,
- calculations of the velocities V_0^t, V_0^n, induced on the airfoil, entries of the vector $\mathbf{B}$ and the product $\mathbf{R}^{-1}\mathbf{B}$ value, respectively, at each time step.

5. Auxiliary velocity field $\vec{V}_A$

The velocity $\vec{V}_A$ written off in the Part I (cf Blażewicz and Styczek, 1993 – Eq (3.20)) remains however the component of a total velocity field and therefore has to be determined.

Having in mind the previous part (cf Błażewicz and Styczek, 1993 – Eq (3.20)) we can write

$$V_A^n = -V_W^n - V_0^n \tag{5.1}$$

where V_W^n, V_0^n denote the normal components of a velocity field induced on the airfoil contour by all the blobs remaining in a flow. After solving equations given in the Part I (cf Błażewicz and Styczek, 1993 – Eq (3.33)) also the youngest generations of blobs may be drawn out. Thus the term $V_A^n(s_l)$ can be calculated at each point of the airfoil using the procedure applied above to the first component of Eq (4.7) calculations (using the induction formula (4.9) and Eq (4.8)).

The tangential component $V_A^t(s_l)$ is calculated in terms of the normal component $V_A^n(s_l)$ as a result of the transformation $\mathcal{L}$ (Błażewicz and Styczek, 1993 – Eq (3.42)). The circumferetial and radial components, respectively, of the velocity V_A on the unit circle located in the auxiliary plane can be denoted by V_θ^A and V_r^A (Blażewicz and Styczek, 1993 – Eqs (3.41) and (3.42)). We can write then

$$V_\theta^A(\theta) = \frac{1}{2\pi} VP \int_0^{2\pi} V_r^A(\varphi) \cot\Big(\frac{\theta}{2} - \frac{\varphi}{2}\Big) d\varphi \tag{5.2}$$

where $V_r^A(\varphi)$ is known.

It is noteworthy that due to the odd and periodic nature of $\cot\alpha$ one obtains

$$VP \int_0^{2\pi} \cot\Big(\frac{\theta}{2} - \frac{\varphi}{2}\Big) d\varphi = 0$$

We can then write

$$V_\theta^A(\theta) = \frac{1}{2\pi} \int_0^{2\pi} \Big[V_r^A(\varphi) - V_r^A(\theta)\Big] \cot\Big(\frac{\theta}{2} - \frac{\varphi}{2}\Big) d\varphi \tag{5.3}$$

It should be marked out that the integral V_θ^A given above has not already been a singular one since the integrand has at the point $\varphi = \theta$ a double sided and finite limit

$$\lim_{\varphi\to\theta}\Big[V_r^A(\varphi)-V_r^A(\theta)\Big]\cot\Big(\frac{\theta}{2}-\frac{\varphi}{2}\Big)=$$

$$=\lim_{\Delta\varphi\to 0}\Big[V_r^A(\theta+\Delta\varphi)-V_r^A(\theta)\Big]\cot\Big(\frac{\theta-\theta-\Delta\varphi}{2}\Big)=$$

$$=-\lim_{\Delta\varphi\to 0}\frac{V_r^A(\theta+\Delta\varphi)-V_r^A(\theta)}{\tan\frac{\Delta\varphi}{2}}=-2\lim_{\Delta\varphi\to 0}\frac{V_r^A(\theta+\Delta\varphi)-V_r^A(\theta)}{\Delta\varphi}=$$

$$=-2\frac{dV_r^A}{d\varphi}\Big|_{\varphi=\theta}$$

Let us calculate the values of V_θ^A at the points θ_l, $l=1,2,...,(NL-1)$. Approximated vales of the derivative are employed to numerical calculations

$$\frac{dV_r^A}{d\varphi}\Big|_{\varphi=\theta_l}\cong\frac{V_r^A(\theta_{l+1})-V_r^A(\theta_{l-1})}{2\Delta\theta}$$

We introduce a new discrete function

$$G(l,i)=\begin{cases}\cot\Big(\frac{\theta_i}{2}-\frac{\varphi_i}{2}\Big) & \text{for } i=0,1,...,NL \quad i\neq l\\ 0 & \text{for } i=l\end{cases}$$

which enables us to establish the integration formula by means of the trapezoidal rule

$$\begin{aligned}V_\theta^A(\theta_l)\ \cong\ & \frac{1}{2\pi}\Big\{\frac{\Delta\theta}{2}\Big[V_r^A(\varphi_0)-V_r^A(\theta_l)\Big]G(l,0)+\\ &+\frac{\Delta\theta}{2}\Big[V_r^A(\varphi_{NL})-V_r^A(\theta_l)\Big]G(l,NL)+\\ &+\Delta\theta\sum i=1^{NL-1}\Big[V_r^A(\varphi_i)-V_r^A(\theta_l)\Big]G(l,i)-\\ &-V_r^A(\theta_{l+1})+V_r^A(\theta_{l-1})\Big\}\qquad l=1,2,...,NL-1\end{aligned}\tag{5.4}$$

The singular case at $\theta=0$ (or $\theta=2\pi$) should be pointed out, for which the integrand is a discontinuous function at $\varphi=0$ and $\varphi=2\pi$, having, like in the case given above, finite limits. We can approximate them as follows

$$\lim_{\varphi\to 0+}\Big[V_r^A(\varphi)-V_r^A(0)\Big]\cot\Big(-\frac{\varphi}{2}\Big)\cong$$

$$\cong-2\lim_{\varphi\to 0+}\frac{V_r^A(\varphi)-V_r^A(0)}{\varphi}=-2\frac{dV_r^A}{d\varphi}\Big|_{0+}\cong-2\frac{V_r^A(\varphi_1)}{\Delta\theta}$$

$$\lim_{\varphi\to 2\pi-}\Big[V_r^A(\varphi)-V_r^A(0)\Big]\cot\Big(-\frac{\varphi}{2}\Big)\cong$$

$$\cong \lim_{\Delta\varphi\to 0}\Big[V_r^A(2\pi-\Delta\varphi)-V_r^A(2\pi)\Big]\cot\Big(-\pi+\frac{\Delta\varphi}{2}\Big)\cong$$

$$\cong \lim_{\Delta\varphi\to 0}\frac{V_r^A(2\pi)-V_r^A(2\pi-\Delta\varphi)}{\Delta\varphi}=-2\frac{dV_r^A}{d\varphi}\Big|_{2\pi-}\cong -2\frac{V_r^A(\varphi_{NL-1})}{\Delta\theta}$$

It can be written then

$$V_\theta^A(0)\cong V_\theta^A(2\pi)=\frac{1}{2\pi}\Big[-V_r^A(\varphi_1)+V_r^A(\varphi_{NL-1})+\Delta\theta\sum_{i=1}^{NL-1}V_r^A(\varphi_i)G(0,i)\Big] \quad (5.5)$$

Thus the formulae (5.4) and (5.5) determine the values of $V_\theta^A(\varphi_l)$ $l=0,1,...,NL$, which enable one, according to the previously given equation (Błażewicz and Styczek, 1993 – Eq (3.41)), to evaluate $V_A^t(s_l)$, $l=1,2,...,NL-1$ on the airfoil. Due to the fact that vanishes at $\theta=0$ the values of $V_A^t(s_0)$ and $V_A^t(s_{NL})$ cannot be calculated using this procedure, which, fortunately, have occured unnecessary.

Finally, applying Eq (2.10) we arrive at the formula for cartesian components of the velocity $\vec{V}_A$ boundary value (evaluated on the airfoil)

$$(u_A-\mathrm{i}v_A)(P_l)=\Big[V_A^t(s_l)-\mathrm{i}V_A^n(s_l)\Big]t^{-1} \quad (5.6)$$

Since the function $V_{Az}(z)=\Big(u_A-\mathrm{i}v_A\Big)(z)$ occurs to be an analytical one in the airfoil exterior and vanishes at the infinity, it can be represented by the Cauchy integral. Employing the similar procedure to the one applied in Part I (Błażewicz and Styczek, 1993) in the formulation of Eq (3.34) we can write

$$V_{Az}(z)=-\frac{1}{2\pi\mathrm{i}}\int_0^{\text{periphery}}\frac{V_{Az}(q)}{q-z}dq=\frac{\mathrm{i}}{2\pi}\int_0^{\text{periphery}}\frac{V_{Az}(q)}{q-z}dq$$

where q stands for the airfoil point and $V_{Az}=u_A-\mathrm{i}v_A$.

The aforementioned formula is valid for the coordinates outside the airfoil. Let us transform the integral given above into the form getting over the problem of the infinite value of V_A^t appearing on the cusp. According to Eq (5.6) and formula given in the Part I (Błażewicz and Styczek, 1993 – Eq (3.41)) we can write

$$V_{Az}=u_A-\mathrm{i}v_A=(V_\theta^A+\mathrm{i}V_r^A)\mathrm{e}^{-\mathrm{i}\beta}\Big(\frac{ds}{d\theta}\Big)^{-1}$$

Having in mind Eq (2.5) one obtains

$$dq=\frac{dz}{d\theta}d\theta=\frac{ds}{d\theta}\mathrm{e}^{\mathrm{i}\beta}d\theta$$

therefore

$$V_{Az}dq = \left(V_\theta^A + \mathrm{i}V_r^A\right)d\theta$$

It can be written

$$V_{Az}(z) = \frac{\mathrm{i}}{2\pi}\int_0^{2\pi}\frac{V_\theta^A + \mathrm{i}V_r^A}{q(\theta) - z}\,d\theta$$

and finally, according to the trapezoidal rule, we can write

$$V_{Az}(z) \cong \frac{\mathrm{i}\Delta\theta}{2\pi}\left[\frac{1}{2}\frac{V_\theta^A(\theta_0) + \mathrm{i}V_r^A(\theta_0)}{P_0 - z} + \frac{1}{2}\frac{V_\theta^A(\theta_{NL}) + \mathrm{i}V_r^A(\theta_{NL})}{P_{NL} - z} + \right. \\ \left. + \sum_{l=1}^{NL-1}\frac{V_\theta^A(\theta_l) + \mathrm{i}V_r^A(\theta_l)}{P_l - z}\right] \tag{5.7}$$

6. Velocity of a blobs convection

The Ito equations describe at each time step the motion of blobs remaining in a flow.

The absolute velocity of a flow can be written in the following form of sum (Blażewicz and Styczek, 1993)

$$\vec{V} = \vec{V}_p + \vec{V}_\Gamma + \vec{V}_A + \vec{V}_W + \vec{V}_0 \tag{6.1}$$

This velocity should be determined at the center of each blob. It is noteworthy, that after having solved some equations given in the Part I (Błażewicz and Styczek, 1993 – Eq (3.33)) all the circulations together with the blobs locations in a flow become known. Let M represent the number of blobs remaining in a flow, B_m denote the center of each blob and Γ_m $(m = 1, 2, ..., M)$ stand for the circulation, respectively.

The first two terms appearing in Eq (6.1) i.e. $\vec{V}_p$ and $\vec{V}_\Gamma$ can be determined by Eqs (3.4) and (3.6), respectively. The circulation appearing in Eq (3.6) is in fact the one, defined in the previous part, where the formula for Γ_C was given (Blażewicz and Styczek, 1993).

Let us assume

$$\Gamma_c = -\sum_{m=1}^{M}\Gamma_m$$

The form of Eqs (3.4) and (3.6) makes it easier to calculate the velocities $\vec{V}_p$ and $\vec{V}_\Gamma$ at the point located on the auxiliary plane, rather than on the flow plane, where the centers of blobs B_m are located. One can calculate the aforementioned

velocities in a simpler way, employing nodes of the network spread over the flow area (being in fact the images of the corresponding network nodes located in the auxiliary plane) and interpolating these values at the points B_m in terms of the already determined at the network nodes ones, respectively.

The linear interpolation has followed the rules given below:

- for each point B_m the network node closest to it should be found together with the two adjacent nodes A and B, in a way ensuring the point B_m to be located within the acute angle ACB area (Fig.5);
- the point E, at which the straight line CB_m intersects the triangle ABC basis AB should be found;
- the linear interpolation rule of velocity should be applied to the segment AB for the value of it to be calculated at the point E;
- the linear interpolation rule of velocity should be applied then to the segment CE for the value of it to be calculated at the point B_m.

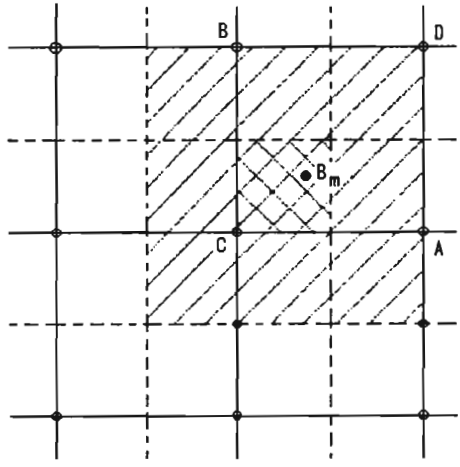

Fig. 5.

The term $\vec{V}_A$ appearing in Eq (6.1) is determined by the formula (5.7) and can be calculated at an arbitrary point of a flow after evaluation of $V_r^A(\theta)$ and $V_\theta^A(\theta)$, respectively, on the unit circle.

Two other terms appearing in Eq (6.1), representing the velocity induced by the high number blobs remaining in a flow need a special treatment due to the time-consuming calculations involved. When the "one-to-one" calculation scheme (permutation scheme) is employed the number of operations to be performed is proportional to M^2, which can be reduced by means of the "indirect" procedure

application. To this end one should calculate first the induced velocities (by all the blobs) at the network nodes and then apply the interpolation rule over the grid for the velocities at the B_m point to be found. This procedure is suitable unless the number of network nodes is greater than the number of blobs.

Unfortunately whenever the sizes of the network mesh are comparable with the sizes of blobs, the the interpolation affects the interaction between the blobs close to each other. It was necessary then to take up the procedure, scheme of which combines both the aforementioned methods i.e. the interpolation over the network mesh and the direct one-to-one scheme. The heart of this method can be established as follows:

the velocity $\vec{V}_0 + \vec{V}_W$ at the point B_m can be represented in the following form of sum

$$\vec{V}_0 + \vec{V}_W = \vec{V}_B + \vec{V}_D \tag{6.2}$$

where $\vec{V}_B$ and $\vec{V}_D$ stand for the velocities induced by the blobs "near" and "distant",respectively, relative the given point B_m, respectively.

The part of a network is shown in Fig.6, with the following point being marked out: B_m and the node C closest to it, two nodes A and B applied to the velocity interpolation at B_m together with the node D completing a quadrilateral mesh (for the sake of simplicity the mesh in Fig.6 is given in the form of squares).

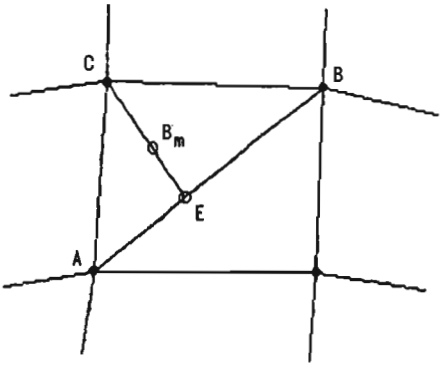

Fig. 6.

For interpolation purposes (also for the motion monitoring simplicity) the following information concerning the blob location are to be found for each blob:

- number of the closest network node C;
- number of the area within which the blob is located i.e one of the four areas surrounding the point C (created by segments connecting C with adjacent nodes).

The aforementioned information (arranged in a proper way) allows us to draw out in a plain way these blobs which appear within one of the four areas surrounding a given node (e.g. the area hatched in Fig.6, close to the point C) and makes it possible to point out all the blobs appearing within the areas adjacent to the chosen one (the area lined in Fig.6).

One can than divide, relative the given point (B_m in Fig.6), all the blobs appearing into two groups "near" – the ones remaining within a lined area and "distant" – the ones lying outside this area.

Using this division we can calculate the value of $\vec{V}_B$ as a sum of velocities induced at the point B_m by the "near" blobs, for which the induction formula (4.9) is to be applied.

The velocity induced by the "distant" blobs should be calculated by means of the indirect method given above, i.e. interpolating the velocity induced at the network nodes in the way given below.

Let us denote the velocity at an arbitrary node as $\vec{V}_{WD}$, which can be calculated as follows

$$\vec{V}_{WD} = \vec{V}_W - \vec{V}_{WB}$$

where

$\vec{V}_W$ – velocity induced at the given node by all the blobs (calculated once at a time step);

$\vec{V}_{WB}$ – velocity induced at the given node by the blobs "near" relative the area, over which the interpolation is performed.

It is obvious that the velocity $\vec{V}_{WD}$ is induced by the blobsnot being the "near" ones. It should also be noticed that it occurred unnecessary to calculate the velocities induced by "almost all" the blobs – i.e. the "distant" ones, for each network mesh, which significantly reduced the calculation costs.

After calculating the term $\vec{V}_0 + \vec{V}_W$ at the point B_m according to Eq (6.2) the conclusion can be made that the velocity of blobs convection has been determined.

7. Numerical results

The simulation procedure described above has been realized in terms of a computer program. Calculations have been done on the IBM PC/AT unit supplied with the Definicon accelerator card, having 4 MB operating memory available. The procedure has been performed for the NACA 0012 (12%) airfoil and the Żukowski airfoil with a slight camber (10%). The results of calculations made for the following four cases are to be presented:

1. flow past the NACA 0012 airfoil at the angle if incidence $\alpha = 6$ degree, velocity at the infinity of which corresponds to the Reynolds number $Re = 2 \cdot 10^6$;

2. flow past the NACA 0012 airfoil at the angle if incidence $\alpha = 6$ degree, $Re = 10^4$;

3. flow past the NACA 0012 airfoil at the angle if incidence $\alpha = 20$ degree, $Re = 10^6$, (see: Part I, Fig. 4 ÷ 6);

4. flow past the Żukowski airfoil at the angle of incidence $\alpha = 2$ degree, $Re = 2 \cdot 10^6$.

The results being obtained consist of the pictures determining in an indirect way the velocity and vorticity fields, respectively. The following results have been obtained:

- arrangement of the blobs within the flow, with the point denoting only the appearance of blob, without giving any information of the vorticity;

- segments of the trajectory of markers having been locatedat an instant at the uniform network spread over the flow nodes and having been observed for some time; equations of these trajectories read

$$\frac{d\vec{r}_p}{dt} = \vec{V}(t, \vec{r}_p) \qquad \vec{r}_p\Big|_{t=t_0} = r_{p0} \tag{7.1}$$

  and have been integrated by means of the Euler method.

The aforementioned images taken at several equidistant instants appear in the form of cycles. Displaying these cycles on the screen in terms of the "picture by picture" scheme one can achieve the animation effect and arrive at the additional information concerning the velocity and vorcity fields creation and evolution, respectively.

Due to the secondary importance and costly calculations the Authors neglected the problem of instantaneous stream lines realization. To this end one would integrate at each instant $t = t_w$ the set of differential equations of type

$$\frac{dx_k}{dl} = u(t_w, x_k, y_k) \qquad \frac{dy_k}{dl} = v(t_w, x_k, y_k) \tag{7.2}$$

which seemed to be both a long-lasting and unnecessary process.

The results averaged with regard to the realization have also been written off due to the low efficiency of the computer unit being employed. Since quasi-periodicity of structures appears explicitly, the ergodicity assumption has also been thrown away. For the quasi-periodicity effects to be filtered out the simulation times long enough are required and thus the calculation time would become longer.

For the reasons given above the results being shown represent the unique realizations of a flow, while the values being presented (time intervals, distances between the vorticity structures) have been obtained upon singular observations, which in a view of stochastic character of the investigated processes, require a cautious judgment.

For approximation purposes of the vorcity boundary distribution, different densities of the airfoil contour division i.e. different sizes and numbers of blobs appearing at one time step have been employed. The following numbers of blobs have been applied to particular cases: 80 blobs in the cases 3 and 4 and 250 blobs in the cases 1 and 2, respectively.

Total numbers of blobs in a flow (being reduced due to the intensity of summing them up) in the aforementioned cases were close to the following values: 3200, 2400, 4100 and 4200, respectively; thus not significantly differed from each other.

Each simulation process started from the irrotational flow field. In the cases 1, 3 and 4, respectively, the velocity at infinity increased from a certain small value to the final one in a relatively short time.

All the results being presented were obtained at instants far from the simulation starting point.

The following effects could be observed in all the cases:

- the area of nonzero vorticity affecting explicitly the velocity field was restricted to the direct vicinity of an airfoil and its wake;

- in the boundary layer (of different thickness on the upper and bottom sides of an airfoil, respectively) made of the drifting and diffusing blobs the vortex structures appear, sizes of which are considerably larger then sizes of the blobs themselves; two different types of these structures can be found looking at the pictures being obtained:

  a) vortices appearing on the airfoil front side (i.e. in the case 3 – close to the airfoil border of attack, in the cases 1 and 2 – approximately at the 1/4 chord length, respectively, and in the case 4 at the 1/3 chord length) and flowing down the airfoil contour towards the trailing edge – Fig.7, 10, 13, 14 and in the previous part, in Fig.8 and 9 particular flow structure detailes are enlarged;

  b) vortices appearing on the airfoil tail, much bigger than the aforementioned ones, which arise in terms of the vortices of the first kind due to the newer ones moving faster and overtaking the vortices, which appeared before thus being able to capture them; the vortex created in such a way is moving slowly or remains fixed and after a while suddenly starts up and flow off the airfoil – Fig.7, 11, 12 and in the previous part;

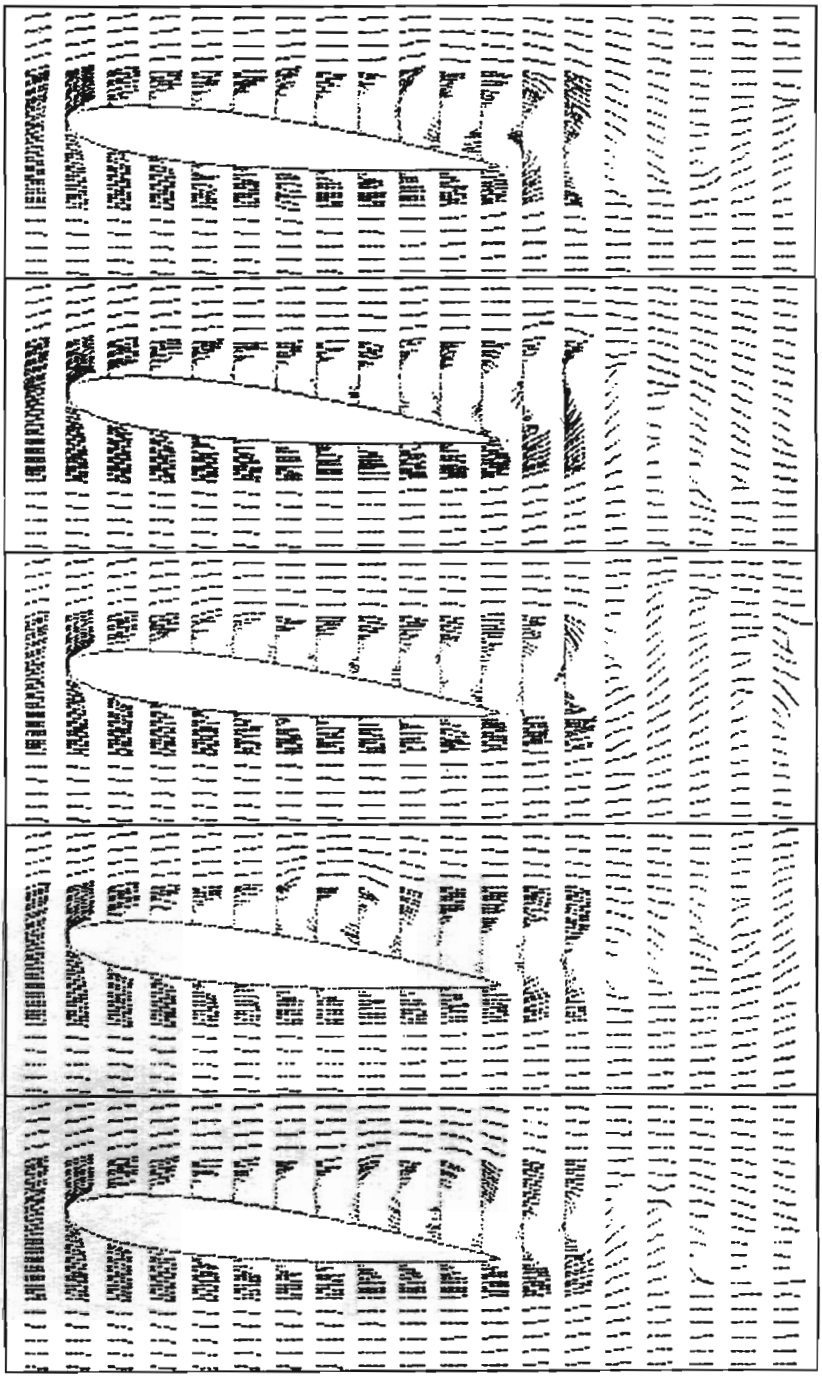

Fig. 7. Flow past the NACA 0012 airfoil; a number of blobs equals approximately 3200, monitoring periods start from 2.3 s, after every 0.15 s, marker paths are registered during the their of motion

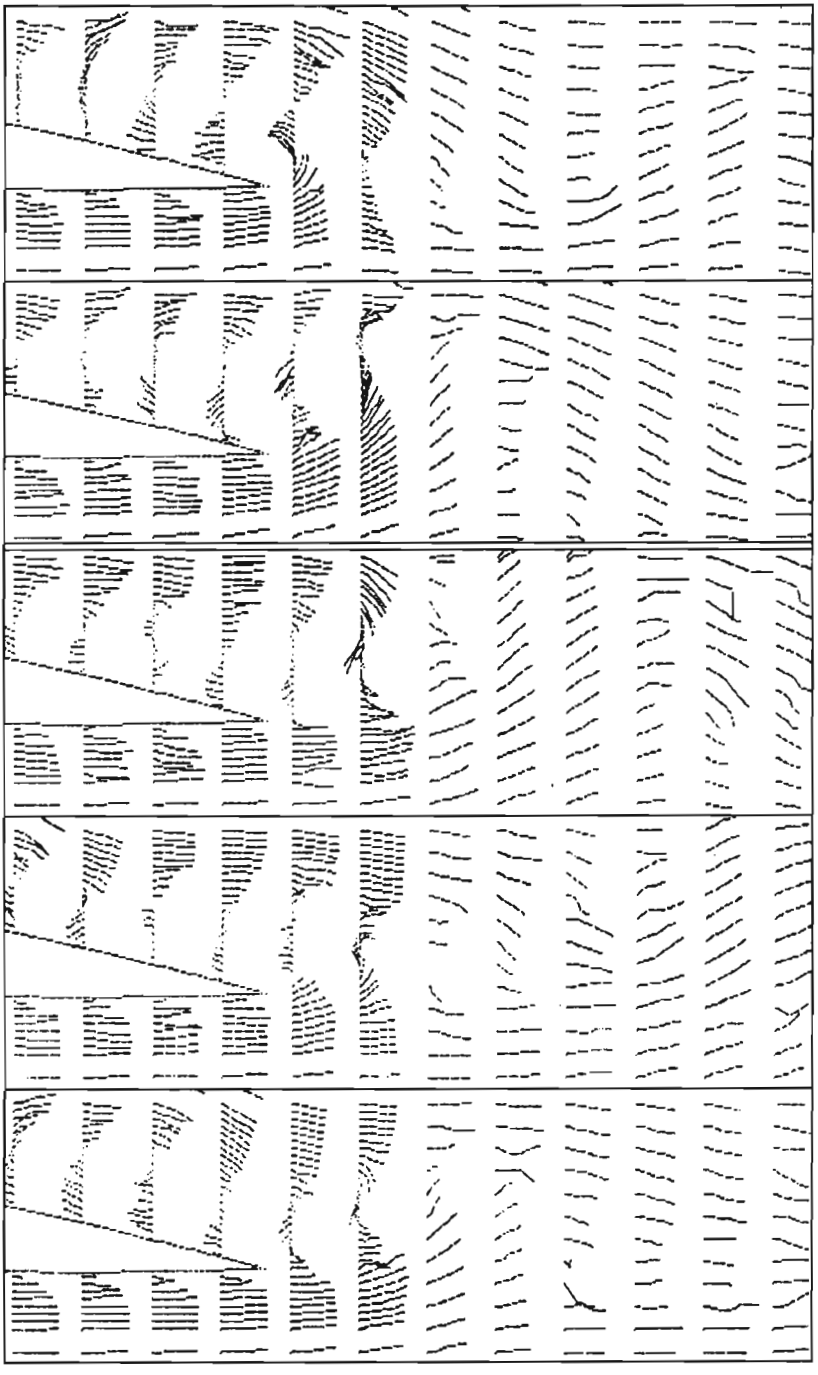

Fig. 8. Parts of the Fig.7 being magnified

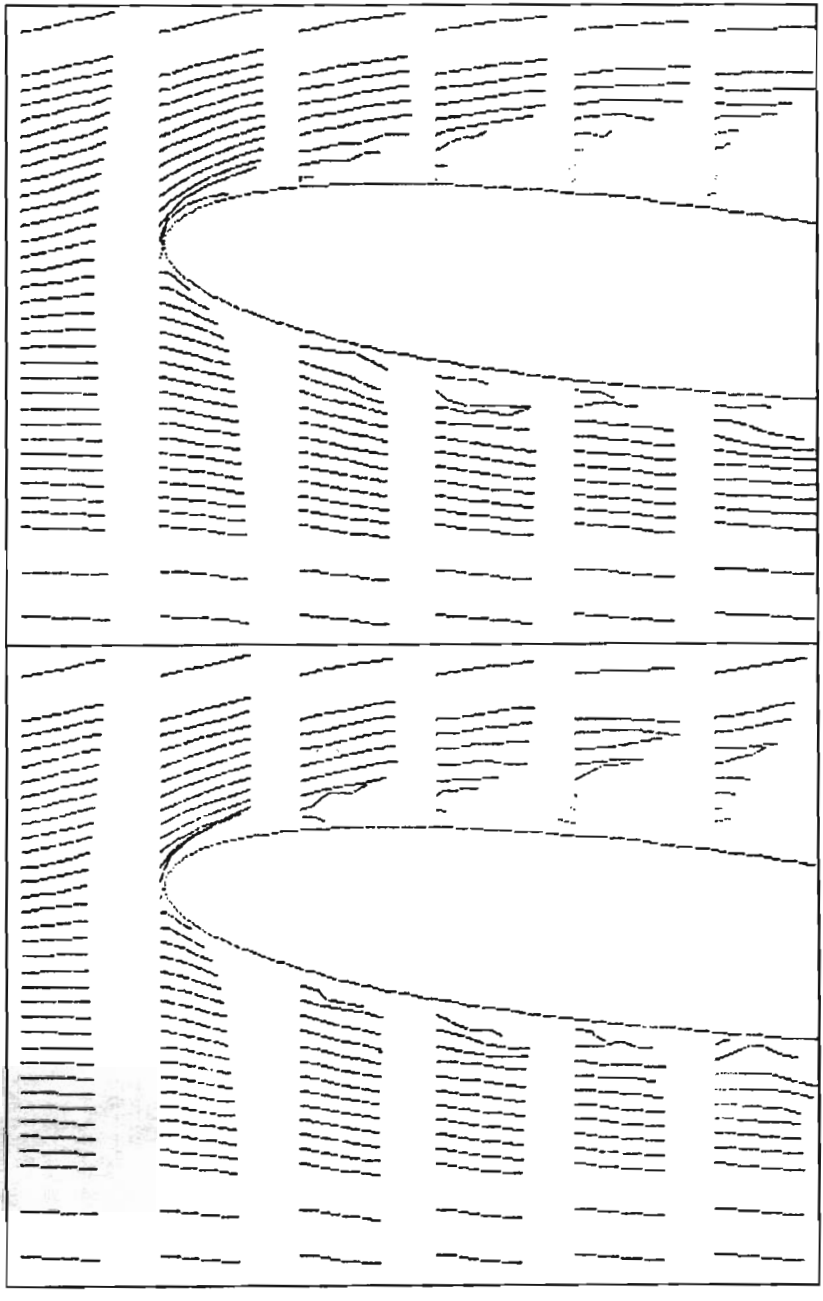

Fig. 9. Scheme of the face airfoil part with the marker paths enclosed, monitoring periods shifted by 0.15 s

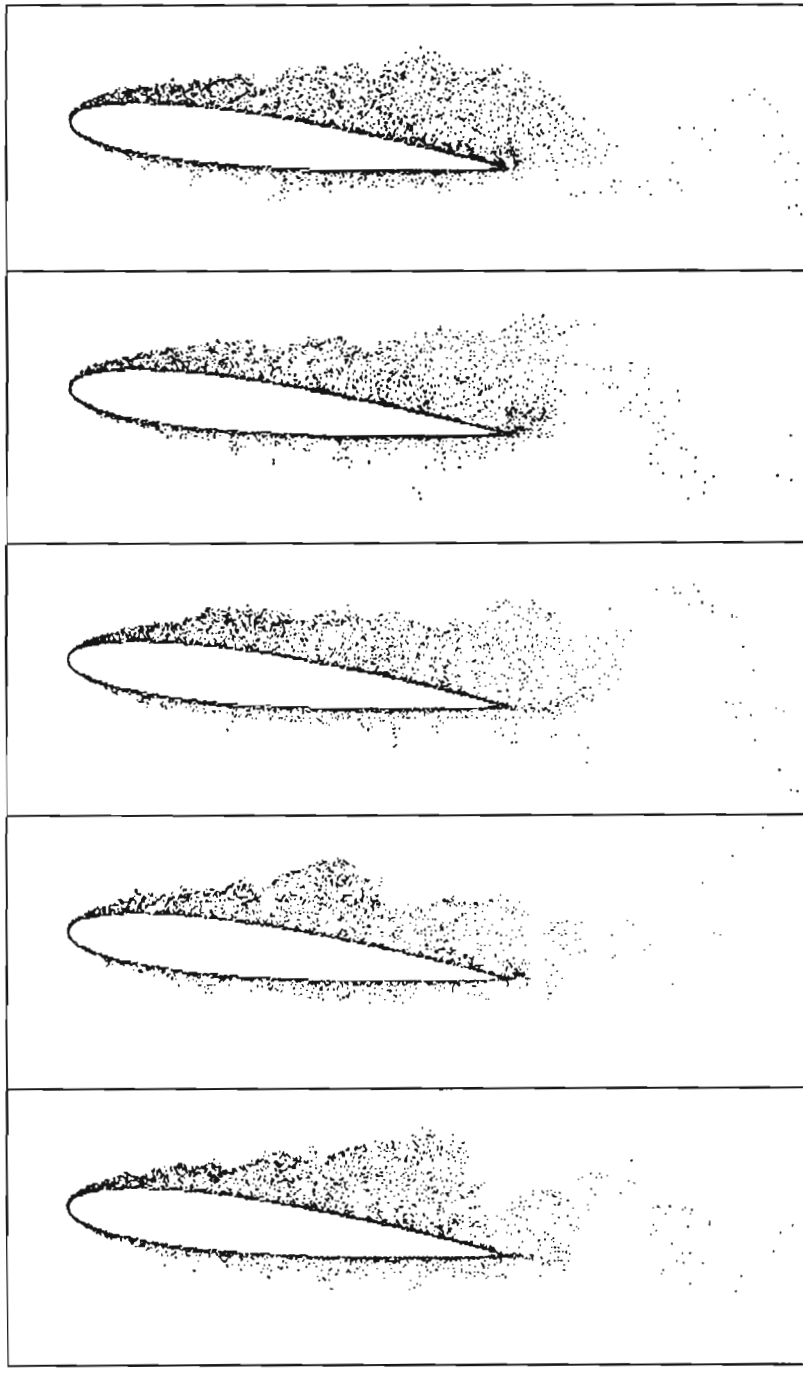

Fig. 10. Instantaneous locations of the blobs centers, with the monitoring periods like in Fig.7

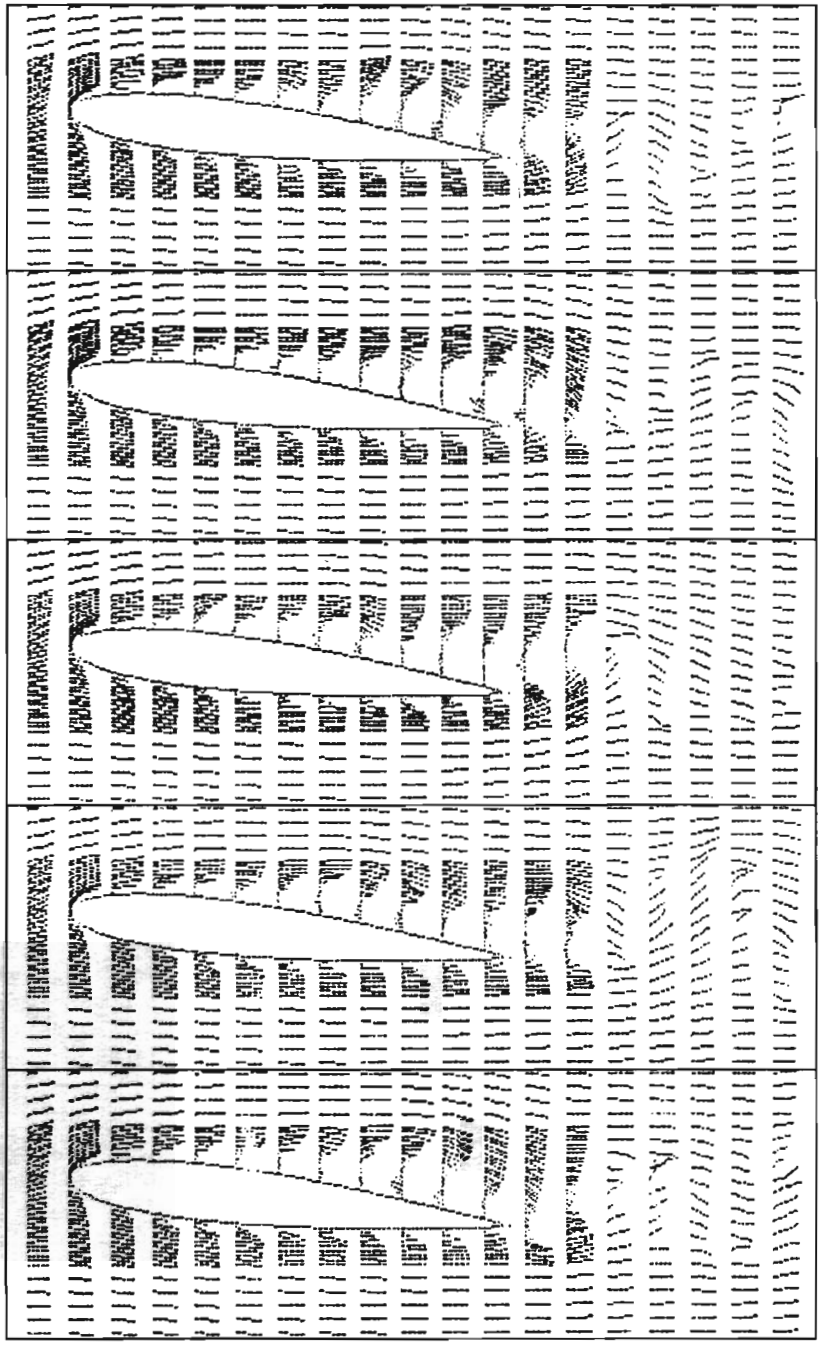

Fig. 11. Flow past the NACA 0012 airfoil; a number of blobs equals approximately 2400, monitoring periods start from 16.4 s, after every 1.64 s, marker paths are registered during the 0.1560 s of motion

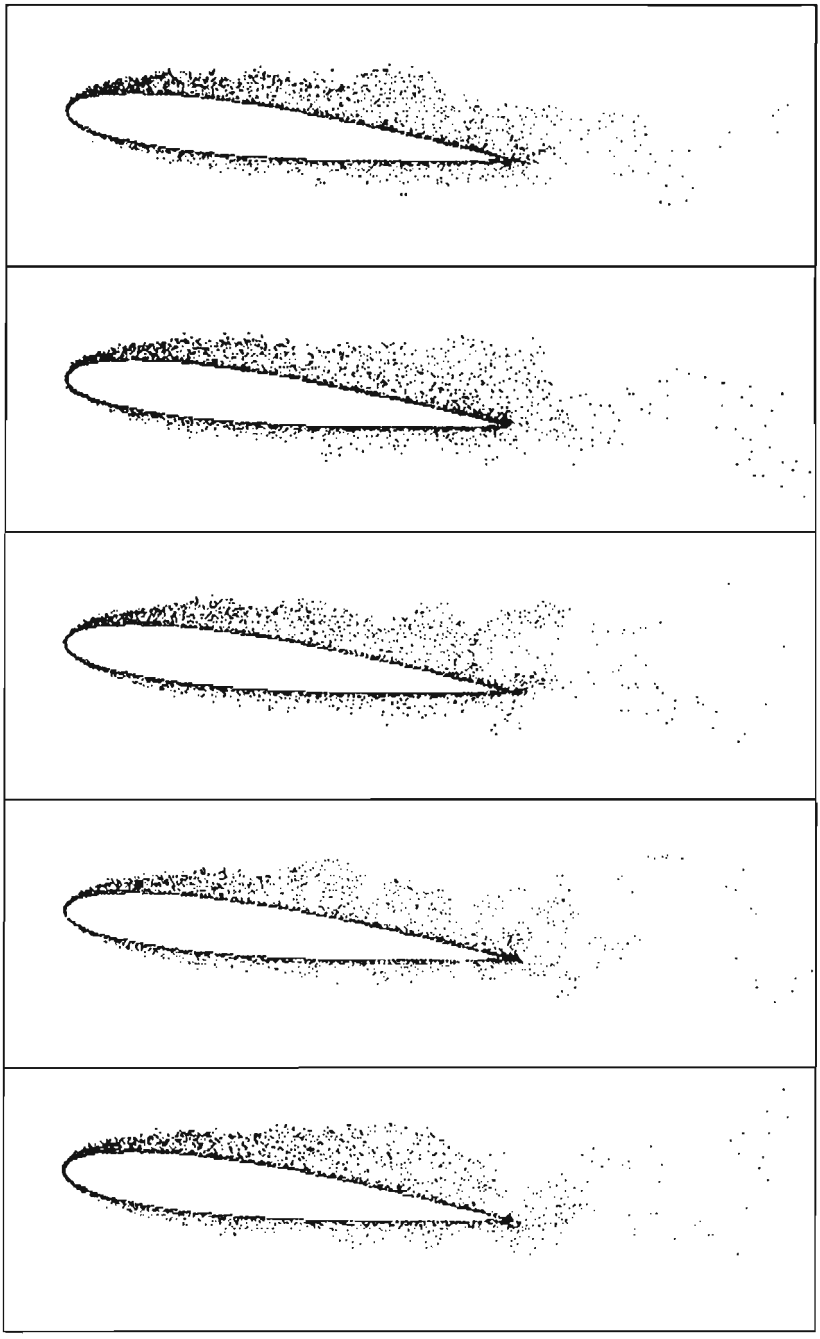

Fig. 12. Instantaneous locations of the blobs centers, with the monitoring periods like in Fig.11

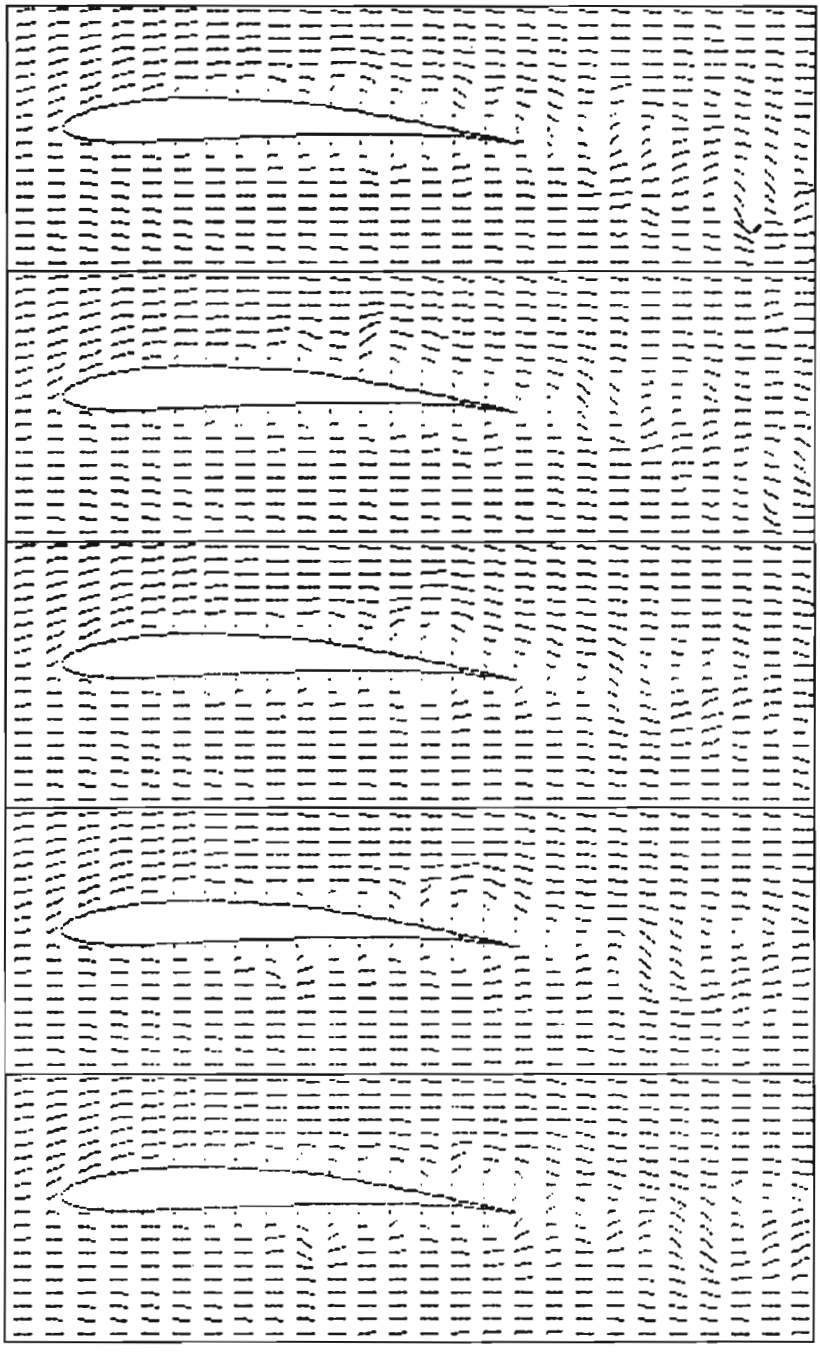

Fig. 13. Flow past the Zukovski airfoil; a number of blobs equals approximately 4200, monitoring periods start from 2.8 s, after every 0.05 s, marker paths are registered during the 0.0192 s of motion

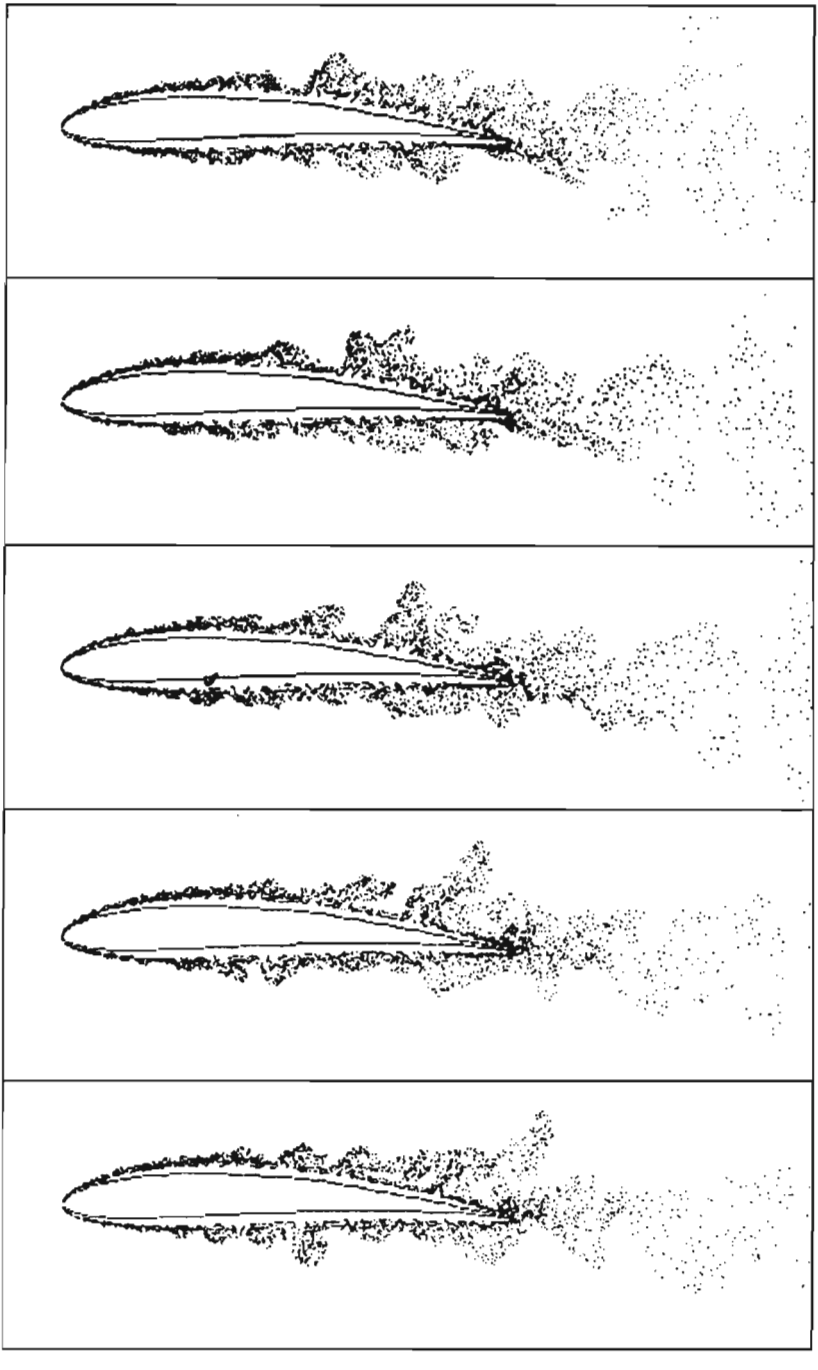

Fig. 14. Instantaneous locations of the blobs centers, with the monitoring periods like in Fig.13

- the airfoil wake displays the properties of an alternate vortices path; distances between the cores reflect the fact that the vortices have been formed due to a cumulation of several vortices of type a), i.e. three of them in the cases 1, 2 and 4, respectively.

Let us determine the Strouhal number connected with the aforementioned structure forming on the vortex path. It can be written as

$$St = \frac{L}{vt^*}$$

where

L – "transverse" size of the airfoil, i.e. the height of the airfoil projection onto a plane perpendicular to the velocity at infinity direction,

vt^* – distance between the wires of the same sign along the vortex path.

Basing on the results being obtained and keeping in mind al the remarks given before and concerning the numerical values of presented quantities, one can calculate the Strouhal number values as:

in the cases 1 and 2 – $St = 0.24$

in the case 4 – $St = 0.20$.

The values given above are close to the ones presented by Gryboś, 1989, for the vortex path behind a cylinder ($St = 0.21$).

A relatively high thickness of the boundary layer should be noticed, being incomparably wider than the one appearing in real flows, which may occur due to big sizes of the blobs employed in simulation. It is known that the sizes of them shall be several times lower than the sizes of structures to be formed. This conclusion may be proved comparing the boundary layer thickness on the airfoil bottom side in the cases 1 and 4, respectively, being in the latter case three times wider than in the first one. It should be stated that for the sake of proper simulation of the effects appearing in a boundary layer the blobs of smaller sizes shall be applied. It is of course possible to increase the number and decrease the sizes of blobs, respectively, but only applying a computer unit of the higher power. Since the calculation were time-consuming the results being obtained were rather expensive, e.g. realization of 400 time steps during calculations of the case 4 (with 80 blobs appearing at each time step) consumed 70 hours, while in the case 1 – 500 time steps (with 250 blobs at each step) consumed 200 hours, respectively. It is obvious that realization of the process with a thousand of blobs at each time step and a total number of them reaching 10 thousand would consume a ten times longer calculation time.

The number and sizes of blobs applied here seem to be sufficient for the modelling of bigger structures purposes i.e. simulation of the boundary layer separation

and the vortex path behind the airfoil, especially in the case of wide angle of attack. So the results given above prove (under the aforementioned limitations) the advantages of the presented method when applied to the viscous flow simulation. The violent progress in the computer technology creates also the promising prospects.

Acknowledgements

The work was financially supported by the KBN Research Project – Grant No. 333149203

References

1. BŁAŻEWICZ J., STYCZEK A., 1993, *The stochastic simulation of a viscous fluid flow past an airfoil – part 1,* J. of Theoretical and Applied Mechanics, 1, **31**
2. GRYBOŚ R., 1989, *Podstawy mechaniki płynów,* PWN, Warszawa
3. PROSNAK W.J., 1970, *Mechanika płynów,* t.I, PWN, Warszawa

Symulacja stochastyczna opływu profilu płynem lepkim – część II, obliczenia numeryczne

Streszczenie

Praca jest kontynuacją artykułu opublikowanego w zeszycie 1/93 MTiS. Zawiera szczegółowy opis algorytmu wynikającego z podanych tam zasad.

Omówione są metody wyznaczania składników zdekomponowanego pola prędkości, metody określenia położenia tworów wirowych i metody wizualizacji komputerowej.

Manuscript received May 17, 1993; accepted for print May 21, 1993